

Document downloaded from the institutional repository of the University of Alcalá: <https://ebuah.uah.es/dspace/>

This is a postprint version of the following published document:

Martínez-López, D. et al. (2021) ' π -Bridge Substitution in DASAs: The Subtle Equilibrium between Photochemical Improvements and Thermal Control', *Chemistry : a European journal*, 27(13), pp. 4420–4429.

Available at <https://doi.org/10.1002/chem.202004988>

© 2020 Wiley-VCH GmbH

(Article begins on next page)



This work is licensed under a
Creative Commons Attribution-NonCommercial-NoDerivatives
4.0 International License.

π -Bridge Substitution in DASAs: the Subtle Equilibrium Between Photochemical Improvements and Thermal Control

David Martínez-López,^[a] Marco Marazzi,^{*[a,b,c]} Cristina García-Iriepa,^{*[b,c]} and Diego Sampedro^{*[a]}

- [a] Dr. D. Martínez-López, Dr. M. Marazzi and Dr. D. Sampedro
Departamento de Química
Centro de Investigación en Síntesis Química (CISQ), University of La Rioja
Madre de Dios, 53, 26006 Logroño, Spain
E-mail: marco.marazzi@uah.es, diego.sampedro@unirioja.es
- [b] Dr. M. Marazzi and Dr. C. García-Iriepa
Department of Analytical Chemistry, Physical Chemistry and Chemical Engineering
Universidad de Alcalá
Ctra. Madrid-Barcelona km 33,600, E-28871 Alcalá de Henares (Madrid), Spain
E-mail: cristina.garciai@uah.es
- [c] Dr. M. Marazzi and Dr. C. García-Iriepa
Chemical Research Institute "Andrés M. del Río" (IQAR)
Universidad de Alcalá
E-28871 Alcalá de Henares (Madrid), Spain

Supporting information for this article is given via a link at the end of the document.

Abstract: Donor–Acceptor Stenhouse Adducts (DASAs) are playing an outstanding role as innovative and versatile photoswitches. Until now, all the efforts have been spent on modifying donor and acceptor moieties, to modulate the absorption energy and improve the cyclization and reversion kinetics. However, there is a strong dependence on specific structural modifications and a lack of predictive behavior, mostly due to the complex photoswitching mechanism. Here, by means of a combined experimental and theoretical study, we systematically explore the effect of chemical modification of the π -bridge linking the donor and acceptor moieties, finding significant impact on the absorption, photocyclization and relative stability of the open form. Especially, a position along the π -bridge is found to be the most suited to red-shift the absorption while preserving cyclization, but affecting reversion. These effects are explained in terms of an increased acceptor capability offered by the π -bridge substituent that can be modulated. This strategy opens the path toward derivatives with infra-red absorption and a potential anchoring point for further functionalization.

Introduction

Molecular photoswitches, that is, molecules that can be interconverted between two states by light, have attracted the attention of scientists in the last decades due to their versatility and outstanding applications.^[1–3] Nevertheless, new families of photoswitches continue to arise aimed mainly at increasing the range of properties and applications. A fascinating example is the emerging Donor–Acceptor Stenhouse Adducts (DASAs), firstly reported by Read de Alaniz in 2014.^[4] DASAs are promising T-type photoswitches characterized by an efficient reversible conversion between a linear triene-colored-hydrophobic and a cyclic-colorless-hydrophilic form (Figure 1).^[5] Different experimental and computational studies have focused on distinct DASAs applications,^[6–12] properties,^[13–15] switching mechanism^[16–20] or reactivity^[21].

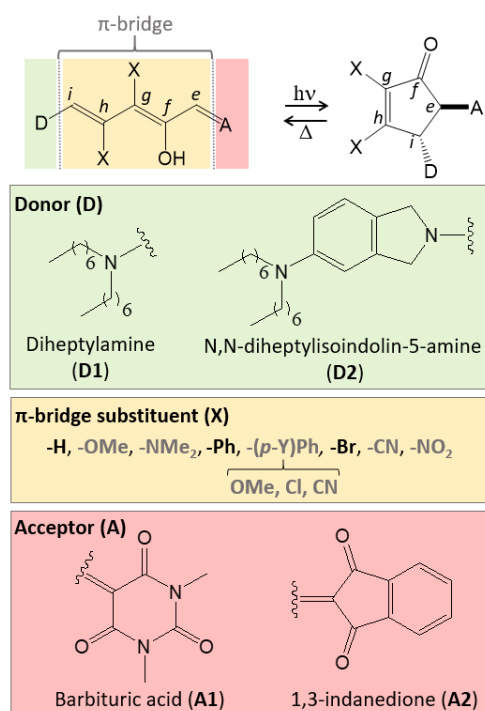


Figure 1. Upper panel: DASAs' overall reactivity. Photoisomerization coupled to cyclization generates the closed form while the extended form is thermally recovered. A general DASA structure is also given including the π -bridge (orange) connecting donor (green) and acceptor (red). Lower panels following the color code: donors, acceptors and π -bridge substituents (in grey if studied only theoretically) investigated in the present work. Theoretical models always include the diethylamino moiety in D, instead of the synthesized diheptylamino moiety.

The photoswitch activation with visible and far-red/near-infrared light is a desired and crucial property for biological and materials applications, as it increases the tissue and surface penetration capability, respectively. So far, several DASAs derivatives absorbing in the visible region have been reported.^[5,22] Different generations of DASAs have been prepared in order to enhance the switchability of these molecules in polar and non-polar media and to red-shift the absorption spectra. It should be remarked

that, up to now, this tunability has been achieved solely by changing two different DASA moieties: acceptor (A) and donor (D) (Figure 1). For instance, it was reported in 2014 that replacing the Meldrum's acid-based acceptor group by a 1,3-indanedione (A2 in Figure 1) results on a red-shift of ca. 50 nm.^[23] Similarly, a second generation of DASAs with an even more red-shifted absorption was proposed by introducing novel aniline-based donors.^[24,25] Recently, a third generation has emerged whose absorption tunability rises from novel structural changes of the carbon acid acceptor.^[22] However, further shifting the absorption wavelength in the infrared region still constitutes a challenge.

Another key aspect of DASAs still poorly understood is the effect that the relative energy of each thermal isomer has on the overall photoswitching process. In contrast with other types of photoswitches, the complete mechanism for DASAs implies a photochemical step for the isomerization of a C=C double bond and several thermal steps that allow for the formation of the final structure, the closed form.^[16,20,26] All these intermediates are in thermal equilibrium and could strongly affect the overall photoswitching process. In turn, the relative stability of these isomers can be modified by several factors. For instance, the effect of the solvent polarity has been deeply studied in these compounds.^[5,15,17,18,22,25] Due to the marked difference in polarity of the open and closed forms, the change in the solvent polarity (for instance going from toluene to acetonitrile) greatly changes the switching process. However, the change in solvent could also affect the relative stability of intermediates, being this fact mainly ignored in previous reports, although changes in the dark equilibrium of these species have been detailed in previous studies. The effect on both switching process and dark equilibrium could be changed not only by the type of solvent, but also by small structural modifications or concentration of the photoswitch.^[13,16,20,25,27]

The basic design features of DASAs have been mainly maintained through the three generations reported. Changes in the D and A moieties have contributed to improve the performance in some cases, but also to the worsening of the photoswitching process or even the complete inactivation of the back reaction.^[5,13,22,28] However, the π -bridge has been kept mainly intact, although it could be considered a potentially relevant modification point. Substitution on the bridge could not only directly alter the relative stability of the different thermally connected isomers, but it also could affect the optical properties and the overall switching process. Even more, substitution at the bridge could be also useful as anchoring point for subsequent functionalization or to bind these compounds in different applications.

In order to increase the knowledge on these systems and test the viability of π -bridge substitution, in this paper we present a comprehensive computational and experimental work mainly focused on the effect of substituting different positions of the π -bridge on the DASAs properties (Figure 1). It was found that DASAs with a modified π -bridge have different absorption properties, photochemical isomerization mechanism and thermal equilibria.

Results and Discussion

The paper is organized as follows. First, the design of several DASAs substituted on the π -bridge is presented. Several positions and functional groups were considered. Next, the

absorption of selected candidates was thoroughly analyzed. One of the main aims for these compounds is the activation using far red or even near infrared light. Then, the photoisomerization was explored. This is the first step in the mechanistic path, and it is related with the potential energy surface in the excited state. Finally, the thermal equilibrium was computed. This final part of the mechanism may be related with the dark equilibria found in these species and responsible for the overall switching process. For all these sections, complementary experimental results will be presented.

Design and synthesis of π -bridge-substituted DASAs

Up to five different positions are, in principle, susceptible for modification in DASAs' π -bridge. The selection of the substitution site among the different possibilities (*e* to *i*, Figure 1) was done based on several mechanistic, synthetic and computational criteria. First, the hydroxyl group in *f* has been shown to be crucial to secure DASA functioning,^[28] hence it was preserved. Second, the typical synthetic route for DASAs, consisting of the opening of a furan ring by the donor moiety, points out the central positions, *g* and *h*, as preferred over the lateral ones, *e* and *i* (Scheme 1). Thus, we initially considered both *g*- and *h*-substituted DASAs from a computational point of view. However, experimentally we aimed for the substitution of furan with Br and Ph to yield *g*-substituted DASAs, as they can be prepared by accessible building blocks and their effect could be relevant enough to change the properties of DASAs. Moreover, both Br and Ph groups could be further functionalized, if required for specific applications.

Preliminary calculations using time dependent-density functional theory (TD-DFT, see Computational Details) were performed to understand the main effects that π -bridge modification could cause on the electronic distribution of these molecules. Beyond this general trend, the nature of the X-substituent group is crucial, since the π -bridge, when unsubstituted, is almost neutral, *i.e.*, it acts as a mere linker between D and A moieties. Nonetheless, appropriate substitutions in this part of the molecule can result in important modifications of the electronic properties of the bridge and, due to this, of the whole DASA. Careful selection of substitution may lead the π -bridge to behave as a D- or A-moiety, hence strikingly increasing the charge transfer character of the $S_0 \rightarrow S_1$ vertical transition. Therefore, we may propose a set of substituents to unveil the chemical nature of the π -bridge, spanning from strong donors (-OMe, -NMe₂) to strong acceptors (-CN, -NO₂), also including substituents with mixed inductive and resonance effects (-Br, -Ph and its derivatives -(*p*-OMe)Ph, -(*p*-Cl)Ph, -(*p*-CN)Ph). In terms of absorption properties and electronic densities, our TD-DFT results surprisingly suggest that the substituted π -bridge acts as an acceptor in all cases. Indeed, when analyzing the $S_0 \rightarrow S_1$ absorption, mainly described by a HOMO \rightarrow LUMO transition, it is evident that the LUMO orbital shows an increased electronic density on the π -bridge group X, even for -NMe₂ (Figure S2). Hence, the π -bridge naturally acts as an acceptor, increasing the overall DASA acceptor ability by coupling through conjugation with the ending A moiety (A1/A2 in Figure 1).

Such electron density displacement toward the newly established acceptor (π -bridge and A1/A2), typical of the S_1 charge transfer character, can be therefore improved by selecting X-substituents with large acceptor strength. Nevertheless, such strength cannot be increased indefinitely: in Figure 2 we compare the calculated charge transfer character of three D2-X-A2 compounds with

increasing X-acceptor strength: $-\text{Br} < -\text{CN} < -\text{NO}_2$. The $-\text{Br}$ derivative already shows how the π -bridge and A form a unified acceptor moiety; in the $-\text{CN}$ derivative the acceptor character is partially displaced toward the π -bridge, maintaining an overall D-A electronic molecular structure; while the $-\text{NO}_2$ derivative results in a D-A-D molecule, since the conventional ending A moiety is converted into a donor. Hence, concerning the photoreactivity, the $-\text{NO}_2$ derivative is expected to behave differently compared to other π -bridge substituted DASAs (see Photoswitching Mechanism section).

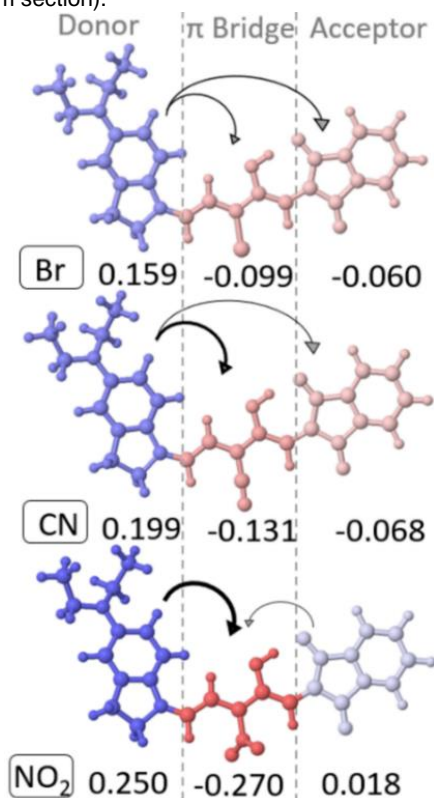
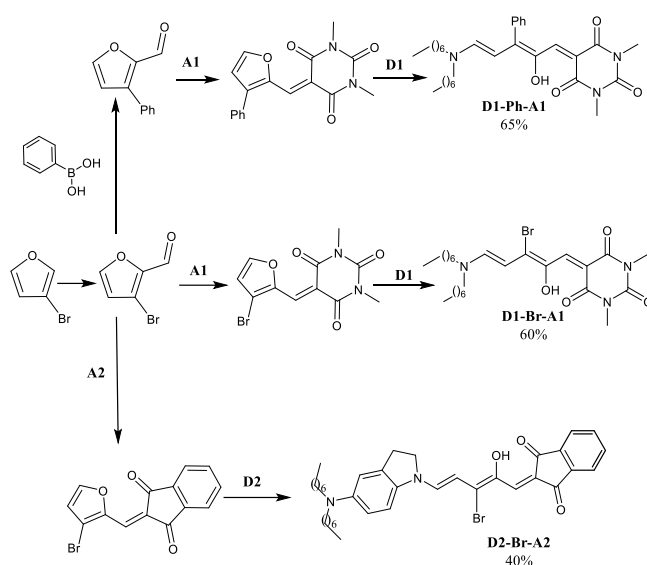


Figure 2. $S_0 \rightarrow S_1$ charge transfer character of $D_2\text{-X-A}_2$ ($X = -\text{Br}, -\text{CN}, -\text{NO}_2$), calculated by TD-DFT (B3LYP/6-31+G(d)) in toluene, applying natural bond order analysis. Electron displacement among the moieties (donor, π -bridge and acceptor) is shown by arrows from positive (blue) to negative (red) regions. The thickness of the arrows is related to the amount of charge transfer.

Inspired by these prospective computational data and within the limits imposed by the acceptor strength of the π -bridge X-substituent, a set of novel DASAs has been synthesized through a modification of the standard procedures^[23,24,29] in order to include π -bridge substituents, as shown in Scheme 1. This implies the preparation of substituted furans that are subsequently opened by the donor moiety to afford the final compounds. A series of DASAs with the general notation D-X-A were prepared in which the donor moiety (D), the acceptor moiety (A) and the π -bridge substituent (X) were modified. Figure 1 includes the structure of the compounds prepared (D: diheptylamine or *N,N*-diheptylisoindolin-5-amine; A: barbituric acid or 1,3-indanedione; X: H, Br or Ph). With this set of compounds in hand, we could determine the effect of every part of the DASA molecule on the different properties.



Scheme 1. Synthetic path for π -bridge substituted DASAs.

Preparation of the unsubstituted DASAs (D-H-A) implies the condensation of furfural with the corresponding acceptor followed by opening of the furan by the donor moiety (see Supporting Information). In contrast, π -bridge substituted compounds require the preparation of the corresponding furan derivative prior to the condensation and ring opening (Scheme 1). To do this, 3-bromofuran was reacted with POCl_3 to prepare the bromofuran carbaldehyde. This compound could be used to prepare the Br-substituted compounds or further reacted under Suzuki conditions to yield 3-phenylfuran-2-carbaldehyde. It is important to note that this synthetic route allows only for the preparation of *g*-substituted compounds. This is due to the regiochemistry in the carbonylation step, in which the aldehyde group is placed in position 2 of the furan while the Br is located in 3 (Scheme 1).

Absorption spectra

A critical feature of photoswitches is the absorption wavelength needed to be activated. This is especially relevant for DASAs as these compounds absorb in the visible region. Careful structural modifications have been used to shift the absorption energy until reaching the red window of the spectrum.^[22,24] This is important for many applications requiring low energy light like, for instance, biological media. A general screening of relevant DASAs including the prepared compounds and additional potential candidates was done through prospective absorption energy calculations. We used the TD-DFT framework, recognized as qualitatively correct in previous DASA studies^[14,15,17,18,20,28] (see Computational Details). Then, the effect of π -bridge substitution was considered. First, we evaluate the effect of X-substitution in both positions *g* and *h*. Our data show that the *g* position leads to more consistent red-shifts compared to the *h* position, especially when increasing the acceptor ability of the X-substituent (Table 1).

Table 1. Absorption energy computed at the B3LYP/6-31+G(d) level of theory for compounds D1-X-A1, considering both the *g* or *h* substitution sites (see Figure 1). The solvent effect (toluene) is applied by polarizable continuum model.

Substituent (X)	Substitution site	Absorption energy eV (nm)
Br	<i>g</i>	2.351 (527)
	<i>h</i>	2.436 (509)
Ph	<i>g</i>	2.398 (517)
	<i>h</i>	2.475 (501)
CN	<i>g</i>	2.299 (539)
	<i>h</i>	2.530 (490)
NO ₂	<i>g</i>	1.931 (642)
	<i>h</i>	2.440 (508)

With the computational absorption spectra and the prepared compounds in hand, we could focus on the effect of the π -bridge X-substituent on DASA absorption properties. In Figure 3 and Table 1 we show both theoretical and experimental results. It should be noted that, to reduce the computational cost, the diheptylamino group in D1/D2 of synthesized DASAs has been replaced by the diethylamino group since, comparing their simulated absorption spectra (Figure S1), only a 5 nm bathochromic shift has been found, due to almost negligible electron density differences.

Regarding the results, a quantitative agreement between the experimental and predicted wavelength at maximum absorbance, λ_{\max} , was achieved by performing calculations with the second-order algebraic diagrammatic construction (ADC(2)) single-configuration reference method. Indeed, on one hand TD-DFT can achieve only a qualitative agreement, with considerable shifts from the experimental value, as shown by our results (Table S2) and previous works on DASAs.^[14] On the other hand, the use of more sophisticated multi-configurational methods is not needed to predict DASA absorption, since it can be described by a single HOMO \rightarrow LUMO transition. Apart from λ_{\max} values, the spectral shape is the other important aspect to reproduce accurately absorption spectra, and this can be properly simulated at TD-DFT level when including the vibrational resolution (Figures S4-S6).¹¹ Hence, we have applied an energy shift to the vibrationally-resolved TD-DFT spectra in order to match the ADC(2) λ_{\max} values (Figure 3b). By applying this computational strategy, a quite good agreement with experiment of both spectral energetics

and shape has been found, with a wide $S_0 \rightarrow S_1$ absorption band characterized by a tail extending to shorter wavelengths.

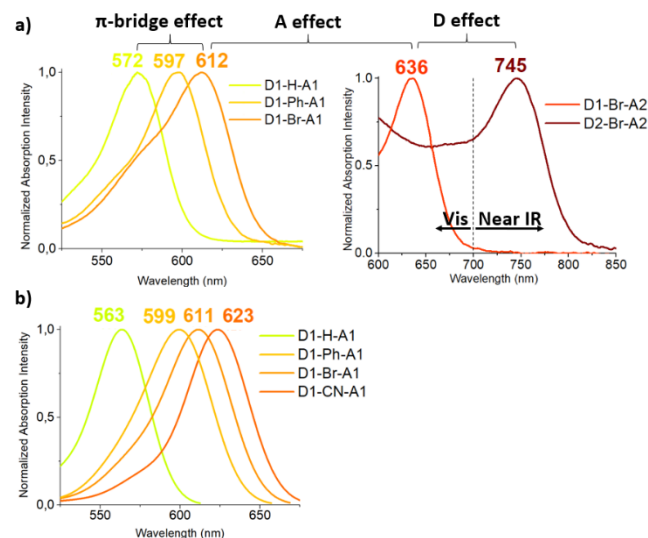


Figure 3. a) Absorption spectra experimentally recorded in toluene, with color code corresponding to λ_{\max} , indicated at the top of each spectrum. Two series are shown, including (left) the effect of the π -bridge substitution in D1-X-A1 (X: -H, -Ph, -Br), and (right) the effect of changing the acceptor (A1 to A2) and the donor (D1 to D2), when X: -Br. b) ADC(2)/DFT spectrum simulation of D1-X-A1 (X: -H, -Ph, -Br, -CN).

Focusing on D1-X-A1 compounds, we observed that by introducing a π -bridge substituent, the absorption spectrum is red-shifted (Table 2 and Figure 3a). In particular, increasing the X-acceptor strength (-Br < -CN < -NO₂) results in an amplified absorption red-shift. The smallest red-shift (~0.1 eV) is induced by -Ph. Due to steric constraints, it is placed almost orthogonal to the π -bridge (Figure S6B), hence considerably reducing its resonant effect and mainly acting through its limited inductive effect. This trend is confirmed for D2-X-A2, D1-X-A2 and D2-X-A1 compounds (Table 2). Hence, we demonstrate that by changing the π -bridge X-substituent, irrespective of D and A moieties, a significant red-shift of the absorption can be achieved, reaching 0.21-0.23 eV when considering the most effective -CN (Table S6). As aforementioned, -NO₂ has a quite different electronic distribution that could affect the switching mechanism (*vide infra*). In addition, the red-shift caused by each X-substituent is a constant value, *i.e.* the same shift has been computed for D1-X-A1 and D2-X-A2 families (0.13-0.14 eV for -Ph, 0.14-0.18 for -Br and 0.21-0.23 for -CN). A similar additive effect has been computed for the D and A moieties, reaching a 0.25-0.28 eV red-shift when modifying D1-X-A1 into D2-X-A2, irrespective of the X-substituent (Table S7).

Table 2. Calculated (ADC(2) level, black) and experimentally determined (solvent: toluene, blue) λ_{\max} , given in eV (nm). The coupled effects of different donor D and acceptor A groups, as well as various π -bridge X-substituents, are shown.

π -bridge X:	Donor D1					Donor D2				
	-H	-Ph	-Br	-CN	-NO ₂	-H	-Ph	-Br	-CN	-NO ₂
Acceptor A1	2.20 (563)	2.07 (599)	2.03 (611)	1.99 (623)	1.86 (666)	1.97 (628)		1.79 (692)		
	2.17 (572)	2.08 (597)	2.02 (612)							
Acceptor A2	2.16 (574)		2.02 (614)			1.94 (641)	1.80 (690)	1.78 (695)	1.71 (723)	1.71 (725)
			1.95 (636)					1.66 (745)		

Photoswitching mechanism

Once checked the effect of the π -bridge substituent on the optical properties, the next step in the reaction mechanism is the light-induced photoisomerization of the adequate C=C double bond. To investigate this issue we have calculated, at the TD-DFT level, the excited-state minimum-energy path of **D2-Br-A2**, **D2-CN-A2** and **D2-NO₂-A2** in toluene, through the polarizable continuum model (Figure 4).^[34] As explained in the previous section, the nitro group seriously affects the electronic structure of the molecule. The computed results confirm the expectations: on one hand, **D2-Br-A2** and **D2-CN-A2** reach a planar S₁ minimum, typical of DASA photochemistry.^[26] Indeed, a S₁ energy barrier along the torsion coordinate is expected to connect this minimum with a S₁/S₀ conical intersection corresponding to a 90 degrees twisted structure around the C_g=C_r photoisomerizable bond, constituting the first step toward cyclization. On the other hand, **D2-NO₂-A2** reaches directly an unproductive S₁/S₀ intersection region, corresponding to pyramidalization of the -NO₂ group, hence conferring only photostability (*i.e.* internal conversion) properties to the compound and hampering the photoisomerization (Figures 4 and S3).

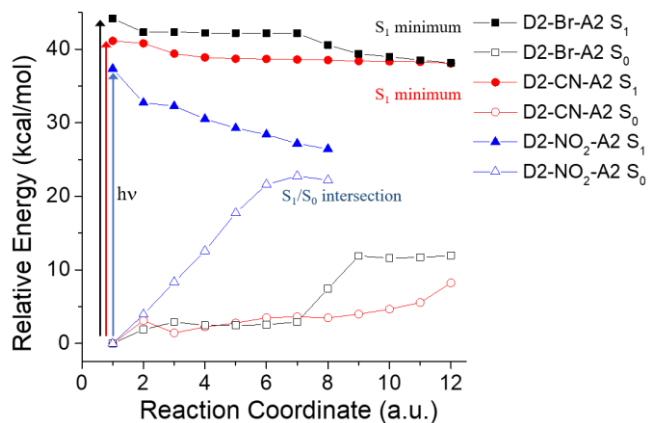
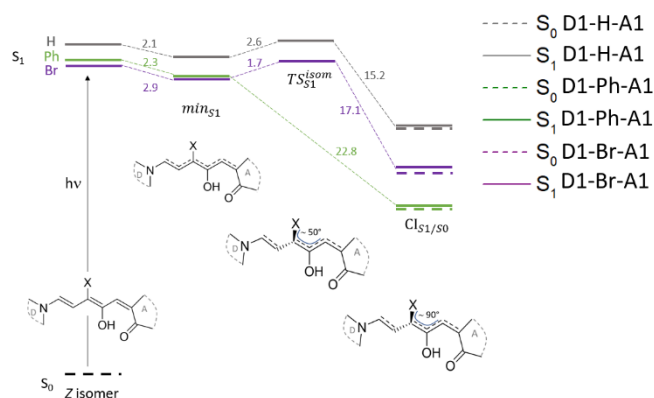


Figure 4. S₁ minimum energy path computed in toluene starting from the Franck-Condon structure (reaction coordinate = 1) at the B3LYP/6-31+G(d) level of theory for the **D2-Br-A2**, **D2-CN-A2** and **D2-NO₂-A2** derivatives. -Br (black) and -CN (red) derivatives reach a planar minimum in the excited state (S₁, full symbols), whereas the -NO₂ derivative reaches an intersection region with the ground state through pyramidalization of the N atom of the -NO₂ group.

To further explore the photochemical part of the mechanism, we computed the key structures along the path for the available experimental compounds (Figure 5). As can be seen, this part of the mechanism is only slightly affected as the main features are maintained for the substituted DASAs. Relevant changes are the red-shift in the absorption spectra and the lowering or even the vanishing of the energy barrier in the excited state which should imply an even faster photoreaction for the π -bridge substituted compounds.

This fast cyclization was experimentally confirmed for all prepared compounds. For instance, upon irradiation on the band maximum of the open **D1-Br-A1**, this compound rapidly isomerizes to the closed form (see Figure 6). This process can be easily followed by UV as the band corresponding to the open form ($\lambda_{\max} = 610$ nm) disappears while the band for the closed form grows.

Figure 5. TD-DFT excited state stationary points along the photochemical reaction path in toluene for the π -bridge (Ph, Br) substituted DASAs at the g



position, compared to unsubstituted DASA (H). Franck-Condon structure (Z isomer), S₁ minimum and S₁ transition state leading to the S₁/S₀ conical intersection (CI) are shown for D1-X-A1.

Hence, we can take advantage of both π -bridge X-substituent and D-A additive effects on the excitation energy, that can be coupled to achieve a further red-shift. Indeed, an infra-red activatable DASA could be finally generated, as shown by our experimental results (**D2-Br-A2** $\lambda_{\max} = 745$ nm in toluene, with a spectral band spanning over 800 nm, see Figure 3a) and as systematically predicted by our ADC(2)//DFT calculations (Table 2). The photocyclability of the newly synthesized DASAs is ensured (see NMR spectra of the closed forms in section 3.1 of Supporting Information) with an excellent red-shifted absorption ($\lambda_{\max} = 695$ nm in toluene),^[22] opening the way to larger red-shifts when considering π -bridge substitutions.

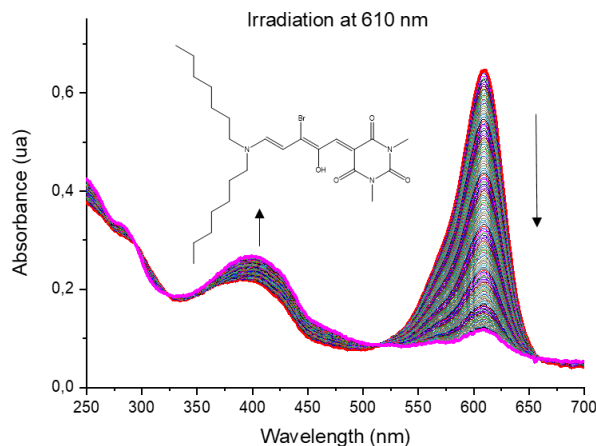


Figure 6. Isomerization of **D1-Br-A1** upon irradiation with 610 nm light in CH₂Cl₂. Conversion was almost quantitative after 4h.

Thermal equilibria

These newly prepared DASAs feature excellent optical properties. Nevertheless, the complete switching mechanism implies not only the formation of the closed form upon irradiation, but also the reversible recovery of the open form under different stimulus, usually thermal activation. This type of switches has been reported to have a marked sensitivity to external factors such as the solvent, but also to slight modifications in their structure.^[5,22] Thus, we then aimed to check the reversibility of these compounds under different stimuli. For all π -bridge substituted compounds D-X-A, the photoreaction from the open to the closed form is performed swiftly under red light. However, these compounds showed no appreciable reversibility back to the

open form even when different reaction conditions were tried. After cyclization, the open form could not be recovered by the use of apolar solvents (toluene, dichloromethane), heating (closed forms were found to be thermally stable at reflux temperature of different solvents) or light (using the wavelength of maximum absorbance, *ca.* 350 nm). These results have two clear implications. First, as these compounds could not be reverted to the initial state, their use as switches is seriously hampered. Second, the thermal part of the switching mechanism is modified somehow by the π -bridge substitution to strongly stabilize the closed form.

In order to further explore these effects, we computed all the ground state stationary points along the complete path for the π -bridge substituted Br and Ph DASAs in both the *g*- and *h*-positions (Figure 7).

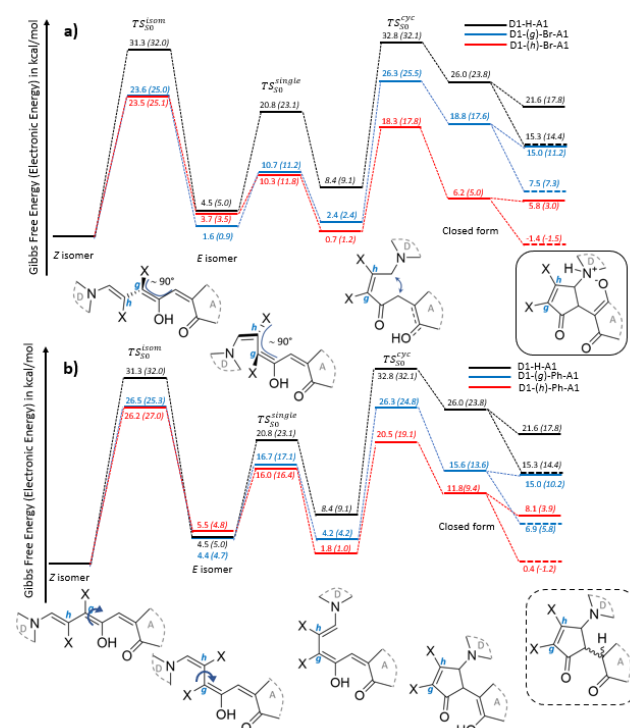


Figure 7. DFT ground state stationary points (minima and connecting transition states) along the mechanistic path for D1-X-A1, computed in toluene. a) Br atom in positions *g* and *h*. b) Ph group in positions *g* and *h*. For comparison purposes, the path computed for the unsubstituted DASA is also shown (black line).

As can be seen, several key aspects are preserved when including substituents in the π -bridge. For instance, the high energy barrier for *Z* / *E* isomerization (thus, requiring light activation) is maintained, although it is reduced by 8 and 5 kcal/mol for the Br and Ph derivatives, respectively. Similarly, the energy barrier for the cyclization is lowered, especially for *h*-substituted compounds. This should imply a faster thermal equilibrium in which the abundance of the different isomers will be controlled by their relative energies, as it was experimentally confirmed by this work. Most of the intermediates are stabilized, especially the final closed forms. For both Br and Ph substituted compounds, there is a clear stabilizing effect, higher for the *h*-substituted compounds. This implies that once formed the closed form, the reverse reaction to the open form will be much slower or even not taking place for the π -substituted compounds, as experimentally found here for the *g*-substituted Br and Ph DASAs. As shown by our computational data, this result could be

extended to the *h*-substituted compounds, although their synthesis was not performed.

Alternatively, especially considering their capacity to be covalently anchored and their solvent dependence, π -bridge substituted DASAs could be proposed as fine-tuned molecular probes or as novel substrate for DASA's reactivity.^[21] Also, depending on the type of closed form that is generated (zwitterionic or non-zwitterionic, see Figure 7), new applications could be envisioned taking advantage of the infrared DASA chemical transformation as a first step of a sequence. An inspirational example could be retinal in visual rhodopsin, where retinal undergoes *cis-trans* photoisomerization within the opsin cavity as a first step, followed by charge migration from retinal to opsin, and requiring replacement of a new retinal molecule within opsin to start a new cycle.^[35] In any case, the detailed mechanistic information gathered here, should be useful in the design of new species and their application in different systems.

Conclusion

We have studied a new generation of DASAs by modifying the π -bridge through chemical substitution at the *g* and *h* positions. Especially, *h* substituted DASAs were investigated only computationally, while the most suitable *g* substituted DASAs were studied both computationally and experimentally. This new π -bridge substituted DASAs can be easily synthesized with high yields and the synthetic path could be straightforwardly modified to get novel analogues or to link these compounds to different substrates. Regarding the optical properties, both the D-A and π -bridge substitution effects were found to be additive to the spectral energy shift, allowing to reach infra-red absorption. More in general, methodology shown here allows to predict from scratch the optical properties of these compounds and their photochemical behavior. The acceptor electronic nature of these π -substituted DASAs was established, including their limit to preserve the photoswitching function.

Clearly, substitution in the π -bridge has profound implications for the properties of DASAs and their switching mechanism. On one hand, a significant and consistent red-shift in the absorption maxima could be achieved. As this effect was found to be additive, substitution in the bridge could be combined with other structural modifications to allow for the use of long wavelengths with these compounds. On the other hand, this specific type of substitution has several limitations that affect the switching process. As shown by the computational results on the $-\text{NO}_2$ derivative, the photoisomerization could be affected if the substituent is not adequately chosen. Even if photoisomerization takes place with a different set of substituents, thermal reversion is compromised.

Results shown herein allow for a detailed description of the behavior of a new set of DASAs. However, further efforts would be necessary to design and prepare different π -bridge compounds that could maintain the excellent optical properties while keeping reasonable switching ability.

Experimental Section

Materials and methods.

All solvents were distilled prior to use. Some solvents such as dichloromethane, diethyl ether, acetonitrile and tetrahydrofuran were distilled with the solvent purification system Pure solvmt 4-MD. Thin Layer chromatography (TLC) was performed using Polygram Sil G/UV254 F254 plates (0,2mm silica gel layer with fluorescence indicator on pre-coated plastic sheets). Column chromatography was carried out with silica gel (230-240 mesh) as stationary phase. Mixtures of hexane/ethyl acetate were used as mobile phase. ^1H and ^{13}C spectra were recorded on a Bruker ARX-300 and/or a Bruker Avance 400 spectrometers. CDCl_3 has been used as the usual deuterated solvent with TMS as internal standard. Chemical shifts are given in ppm and coupling constants in hertz. Absorption molecular spectra were recorded on two distinct equipment: HP-8453A UV-VIS-NIR diode array spectrophotometer (190-1100 nm) or HP 8451A diode array spectrophotometer (190-820 nm). All the experiments were carried out in quartz cuvettes (1 cm path length). Electrospray mass spectra were recorded on a HP 5989B mass spectrometer with an HP59987A interface in positive-ion mode. High resolution mass spectrometry was performed in a HP Bruker Microtof-Q with an Apollo II electrospray source in positive-ion mode.

Synthesis and Characterization of D1-Br-A1

Barbituric acid (3 mmol, 470 mg, 1 equiv.) and 3-bromofuran-2-carbaldehyde (3.3 mmol, 580 mg, 1.1 equiv.) were dissolved in water and reacted at 70° C for 2 hours. After that, the reaction was cooled to rt and the solid was isolated by filtration. The product did not need further purification and could be used immediately in the next step.

The adduct (0.1 mmol, 31.3 mg, 1 equiv.) was dissolved in THF at 0°C, then diheptylamine (0.11 mmol, 23.43 mg, 1.1 equiv.) was added dropwise. Promptly, the solution changed its color from yellow to blue-purple. The reaction was stirred for additional 15 minutes. The final compound was purified by HPLC, using a different linear gradient 95-0% water (containing 0.1% TFA) / acetonitrile over a period of 30 minutes. ^1H NMR (300 MHz, Methanol- d_4) δ 7.91 (d, J = 2.3 Hz, 1H), 4.81 (dd, J = 3.6 Hz, J = 2.3 Hz, 1H), 3.94 (d, J = 3.6 Hz, 1H), 3.23 (m, 10H), 1.66 (m, 4H), 1.29 (m, 16H), 0.90 (m, 6H). ^{13}C NMR (75 MHz, MeOD) δ (ppm) 198.6, 164.9, 154.6, 151.3, 132.8, 85.3, 67.8, 45.3, 32.7, 29.9, 29.8, 28.1, 27.5, 27.4, 27.3, 23.6, 14.4. UV-VIS (CH_2Cl_2 , open form): λ (nm) 610 (ϵ = 15768 $\text{M}^{-1}\text{cm}^{-1}$). EM-ES (+): calcd for $\text{C}_{25}\text{H}_{41}\text{N}_3\text{O}_4\text{Br}$ [M^+ H] $^+$ 526.2280, found 526.2275.

Synthesis and Characterization of D2-Br-A2

1,3-indandione (1 mmol, 132 mg, 1 equiv.) was dissolved in water. To this solution, 3-bromofuran-2-carbaldehyde (1.1 mmol, 175 mg, 1.1 equiv.) was added dropwise and then, the mixture was heated at 70°C for 2 hours. After that, the reaction was cooled to rt, and the resulting precipitate was filtered and used without further purification. This adduct (0.1 mmol, 30 mg, 1 equiv.) was dissolved in THF at 0°C, then *N,N*-diheptylindolin-5-amine (0.11 mmol, 36 mg, 1.1 equiv.) was added dropwise. Promptly, the solution changed its colour from yellow to blue-purple. The reaction was stirred for additional 15 minutes. The final compound was purified by HPLC, using a different linear gradient 95-0% water (containing 0.1% TFA) / acetonitrile over a period of 30 minutes. ^1H NMR (300 MHz, Methanol- d_4) δ 8.07 (d, J = 7.9 Hz, 1H), 8.01 (dd, J = 6.7, 1.8 Hz, 1H), 7.97 (s, 1H), 7.92 (s, 2H), 7.25 (s, 1H), 6.96 (s, 1H), 6.47 (d, J = 8.6 Hz, 1H), 5.30 (s, 1H), 3.75 (s, 1H), 3.70 (s, 1H), 3.51 (s, 6H), 3.14 (s, 2H), 1.51 (s, 4H), 1.29 (s, 16H), 0.90 (s, 6H). ^{13}C NMR (75 MHz, Methanol- d_4) δ 200.5, 199.2, 198.0, 162.1, 152.9, 144.0, 143.1, 137.3, 137.0, 134.5, 128.8, 126.9, 124.3, 123.9, 122.8, 119.1, 107.5, 60.3, 60.1, 47.3, 32.6, 29.8, 28.8, 27.2, 26.2, 23.5, 14.3. UV-VIS (CH_2Cl_2 , open form): λ (nm) 750 (ϵ = 15033 $\text{M}^{-1}\text{cm}^{-1}$). EM-ES (+): calcd for $\text{C}_{36}\text{H}_{46}\text{BrN}_2\text{O}_3$ [M^+ H] $^+$ 633.2692, found 633.2686.

Computational Methods

Ground state stationary points of all compounds were optimized on the ground state at the B3LYP^{[36,37]/6-31+G(d)} level of theory, followed by a frequency calculation to ensure that the optimized structure corresponds to a minimum or a transition state on the S_0 potential energy surface. As mentioned in the text, both TD-DFT and ADC(2)^[38] calculations were performed to describe excited state properties, being the former only qualitatively correct, while the latter can be also quantitatively compared with the experiment. Concerning the TD-DFT calculations, a benchmark was performed on **D1-Br-A1**, finding out that the B3LYP functional can be used also for excited state calculations (Table S1). The effect of the basis set on the absorption energy was also benchmarked, finally selecting the 6-31+G(d) basis set (Table S2). The intramolecular charge transfer in D2-(g)X-A2 compounds, during irradiation, was analyzed by Natural Bond Order (NBO) analysis^[39] at the B3LYP/6-31+G(d) level of theory, including toluene as solvent (Figure 2 and Table S3). In order to perform more affordable calculations, the diheptylamino moiety of synthesized compounds was substituted with the diethylamino one, showing for **D2-(g)Br-A2** how this modifications affects only negligibly the overall absorption spectrum (Figure S1). The shape of the absorption spectra was modeled at B3LYP/6-31+G(d) level including the vibrationally-resolved resolution,^[30–33] in order to match the experimental shape, as suggested elsewhere^[14] (Figures S4-S6). The ground state and excited state stationary points shown in Figures 5 and 7 have been also computed with the M062X functional (Figures S8 and S9), validating the general trend found with the B3LYP functional.

Concerning ADC(2) calculations of the absorption spectrum, a basis set benchmark was performed, showing that convergence can be reached only when employing the aug-cc-pVTZ (Table S4). Also, the contribution of single and double excitations was checked by ADC(2) molecular orbital analysis (Figure S7 and Table S5), showing a small but non-negligible participation of double excitations, that could suggest the discrepancy in λ_{max} values between TD-DFT and ADC(2) methods, although maintaining a correct description of the electronic nature.

Solvent effects were taken into account by the Polarizable Continuum Model using the Integral Equation Formalism variant (IEF-PCM).^[40,41]

All DFT and TD-DFT calculations were performed with the Gaussian16^[42] suite of programs, while ADC(2) calculations were carried out with the Turbomole 7.3^[43] program.

Acknowledgements

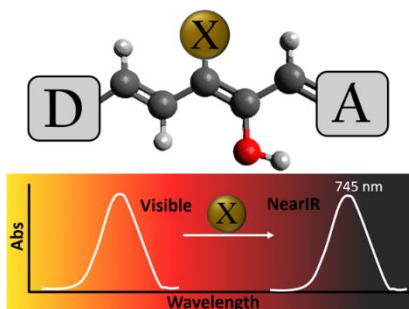
This research was supported by the MINECO/FEDER (CTQ2017-87372-P). D. M.-L. and M. M. are grateful to Universidad de La Rioja for a doctoral and a postdoctoral fellowship, respectively.

Keywords: DASA • photochemistry • thermal equilibrium • photoswitches

- [1] W. Browne, B. Feringa, *Molecular Switches*, Wiley Online Library, 2011.
- [2] D. Bléger, S. Hecht, *Angew. Chemie Int. Ed.* **2015**, *54*, 11338–11349.
- [3] C. García-Iriepa, M. Marazzi, L. M. Frutos, D. Sampedro, *RSC Adv.* **2013**, *3*, 6241–6266.
- [4] S. Helmy, F. Leibfarth, S. Oh, J. Poelma, *J. Am. Chem. Soc.* **2014**, *136*, 8169–8172.
- [5] M. M. Lerch, W. Szymański, B. L. Feringa, *Chem. Soc. Rev.* **2018**, *47*, 1910–1937.
- [6] O. Rifaie-Graham, S. Ulrich, N. F. B. Galensowske, S. Balog, M. Chami, D. Rentsch, J. R. Hemmer, J. Read De

- Alaniz, L. F. Boesel, N. Bruns, *J. Am. Chem. Soc.* **2018**, *140*, 8027–8036.
- [7] R. Saha, A. Devaraj, S. Bhattacharyya, S. Das, E. Zangrando, P. S. Mukherjee, *J. Am. Chem. Soc.* **2019**, *141*, 8638–8645.
- [8] A. Belhboub, F. Boucher, D. Jacquemin, *J. Mater. Chem.* **2017**, *5*, 1624–1631.
- [9] S. Ulrich, J. Hemmer, Z. Page, N. Dolinski, *ACS Macro Lett.* **2017**, *6*, 738–742.
- [10] J. E. Yap, N. Mallo, D. S. Thomas, J. E. Beves, M. H. Stenzel, *Polym. Chem.* **2019**, *10*, 6515–6522.
- [11] S. Jia, A. Tan, A. Hawley, B. Graham, B. J. Boyd, *J. Colloid Interface Sci.* **2019**, *548*, 151–159.
- [12] Y. De Cai, T. Y. Chen, X. Q. Chen, X. Bao, *Org. Lett.* **2019**, *21*, 7445–7449.
- [13] N. Mallo, E. D. Foley, H. Iranmanesh, A. D. W. Kennedy, E. T. Luis, J. Ho, J. B. Harper, J. E. Beves, *Chem. Sci.* **2018**, *9*, 8242–8252.
- [14] A. Laurent, M. Medved', D. Jacquemin, *ChemPhysChem* **2016**, *17*, 1846–1851.
- [15] C. García-Iriepa, M. Marazzi, *Materials (Basel)*. **2017**, *10*, 1025.
- [16] J. N. Bull, E. Carrascosa, N. Mallo, M. S. Scholz, G. Da Silva, J. E. Beves, E. J. Bieske, *J. Phys. Chem. Lett.* **2018**, *9*, 665–671.
- [17] M. M. Lerch, M. Di Donato, A. D. Laurent, M. Medved', A. Iagatti, L. Bussotti, A. Lapini, W. J. Buma, P. Foggi, W. Szymański, et al., *Angew. Chemie - Int. Ed.* **2018**, *57*, 8063–8068.
- [18] M. Di Donato, M. M. Lerch, A. Lapini, A. D. Laurent, A. Iagatti, L. Bussotti, S. P. Ihrig, M. Medved', D. Jacquemin, W. Szymański, et al., *J. Am. Chem. Soc.* **2017**, *139*, 15596–15599.
- [19] M. Lerch, S. Wezenberg, W. Szymanski, *J. Am. Chem. Soc.* **2016**, *138*, 6344–6347.
- [20] H. Zulfikri, M. A. J. Koenis, M. M. Lerch, M. Di Donato, W. Szymański, C. Filippi, B. L. Feringa, W. J. Buma, *J. Am. Chem. Soc.* **2019**, *141*, 7376–7384.
- [21] J. Alves, S. Wiedbrauk, D. Gräfe, S. L. Walden, J. P. Blinco, C. Barner-Kowollik, *Chem. - A Eur. J.* **2020**, *26*, 809–813.
- [22] J. R. Hemmer, Z. A. Page, K. D. Clark, F. Stricker, N. D. Dolinski, C. J. Hawker, J. Read De Alaniz, *J. Am. Chem. Soc.* **2018**, *140*, 10425–10429.
- [23] S. Helmy, S. Oh, F. A. Leibfarth, C. J. Hawker, J. Read de Alaniz, *J. Org. Chem.* **2014**, *79*, 11316–11329.
- [24] J. Hemmer, S. Poelma, N. Treat, *J. Am. Chem. Soc.* **2016**, *138*, 13960–13966.
- [25] N. Mallo, P. T. Brown, H. Iranmanesh, T. S. C. MacDonald, M. J. Teusner, J. B. Harper, G. E. Ball, J. E. Beves, *Chem. Commun.* **2016**, *52*, 13576–13579.
- [26] C. García-Iriepa, M. Marazzi, D. Sampedro, *ChemPhotoChem* **2019**, *3*, 866–873.
- [27] B. F. Lui, N. T. Tierce, F. Tong, M. M. Sroda, H. Lu, J. Read De Alaniz, C. J. Bardeen, *Photochem. Photobiol. Sci.* **2019**, *18*, 1587–1595.
- [28] M. M. Lerch, M. Medved, A. Lapini, A. D. Laurent, A. Iagatti, L. Bussotti, W. Szymański, W. J. Buma, P. Foggi, M. Di Donato, et al., *J. Phys. Chem. A* **2018**, *122*, 955–964.
- [29] S. P. Meth-Cohn, O.; Stanforth, in *Compr. Org. Synth.* (Ed.: I. Trost, B. M.; Fleming), Pergamon: Oxford, **1991**, pp. 777–794.
- [30] F. Santoro, R. Improta, A. Lami, J. Bloino, V. Barone, *J. Chem. Phys.* **2007**, *126*, 084509.
- [31] F. Santoro, A. Lami, R. Improta, V. Barone, *J. Chem. Phys.* **2007**, *126*, 184102.
- [32] G. Herzberg, E. Teller, *Phys. Chem. B* **1933**, *21*, 410.
- [33] G. J. Small, *J. Chem. Phys.* **1971**, *54*, 3300–3306.
- [34] J. Tomasi, B. Mennucci, R. Cammi, *Chem. Rev.* **2005**, *105*, 2999–3093.
- [35] M. Marazzi, C. Garcia-Iriepa, *Retin. Inspired Photoswitches From Isomerization Mech. Towar. Recent Appl. Photoisomerization Causes, Behav. Eff.* **2019**, 189–238.
- [36] A. D. Becke, *J. Chem. Phys.* **1993**, *98*, 1372–1377.
- [37] C. Lee, W. Yang, R. G. Parr, *Phys. Rev. B* **1988**, *37*, 785–789.
- [38] C. Hättig, A. Köhn, *J. Chem. Phys.* **2002**, *117*, 6939–6951.
- [39] F. Weinhold, C. R. Landis, *Valency and Bonding: A Natural Bond Orbital Donor–Acceptor Perspective*, **2005**.
- [40] J. L. Pascual- ahuir, E. Silla, I. Tuñon, *J. Comput. Chem.* **1994**, *15*, 1127–1138.
- [41] M. Cossi, V. Barone, R. Cammi, J. Tomasi, *Chem. Phys. Lett.* **1996**, *255*, 327–335.
- [42] G. E. S. M. J. Frisch, G. W. Trucks, H. B. Schlegel, V. B. M. A. Robb, J. R. Cheeseman, G. Scalmani, A. V. M. G. A. Petersson, H. Nakatsuji, X. Li, M. Caricato, H. P. H. J. Bloino, B. G. Janesko, R. Gomperts, B. Mennucci, D. W.-Y. J. V. Ortiz, A. F. Izmaylov, J. L. Sonnenberg, A. P. F. Ding, F. Lipparini, F. Egidi, J. Goings, B. Peng, N. R. T. Henderson, D. Ranasinghe, V. G. Zakrzewski, J. Gao, R. F. G. Zheng, W. Liang, M. Hada, M. Ehara, K. Toyota, H. N. J. Hasegawa, M. Ishida, T. Nakajima, Y. Honda, O. Kitao, J. E. P. T. Vreven, K. Throssell, J. A. Montgomery, Jr., et al., **2016**.
- [43] *TURBOMOLE V7.3*, 2018, A Development Of University Of Karlsruhe And Forschungszentrum Karlsruhe GmbH, 1989–2007, TURBOMOLE GmbH, Since 2007; Available From [Http://www.turbomole.com](http://www.turbomole.com)., **2018**.

Entry for the Table of Contents



A new set of Donor-Acceptor Stenhouse adducts was computationally studied and prepared through the substitution on the π -bridge. This allows for the modification of absorption, photocyclization and relative stability of the isomers. This change provides a consistent red-shift in the absorption maximum and a structural entry point for subsequent derivatization, although the reversibility is affected.